JOURNAL OF SOLID STATE CHEMISTRY 84, 355–364 (1990)

# A Structural Investigation of $Ag_{0.167}TiS_2$ by Time-of-Flight Neutron Powder Diffraction

G. L. BURR, V. G. YOUNG, JR., M. J. MCKELVY AND W. S. GLAUNSINGER*

*Department of Chemistry and Center for Solid State Science, Arizona State University, Tempe, Arizona 85287-1604*

AND R. B. VON DREELE

*Los Alamos Neutron Scattering Center, MS-H805, Los Alamos National Laboratory, Los Alamos, New Mexico 87545*

Received August 7, 1989; in revised form October 16, 1989

The structure of $Ag_{0.167}TiS_2$ has been determined at several temperatures from time-of-flight neutron powder diffraction data. At 305 K, $Ag_{0.167}TiS_2$ is a stage-II complex which belongs to the space group $P\bar{3}m1$, with $a = 3.4161(4)$ Å and $c = 12.100(2)$ Å. When the temperature is lowered to 13 K, the lattice parameters decrease, but no phase change or superlattice formation is observed. Upon heating to 1123 K, this compound transforms to a stage-I structure belonging to the space group $P\bar{3}m1$, with $a = 3.4676(1)$ Å and $c = 6.2247(4)$ Å. No further phase changes are observed when the temperature is raised to 1323 K. When this compound is slowly cooled to ambient temperature from 1323 K, it transforms quantitatively to the original stage-II structure. The Rietveld refinements of $Ag_{0.167}TiS_2$ at six temperatures are presented and discussed. 

## Introduction

During the past two decades, lamellar transition metal dicalcogenides intercalated with various metals have been studied intensively (*1–3*). These intercalation compounds, $M_xTX_2$ (where $M$ is the intercalated metal, $T$ is the transition metal, and $X$ is either S or Se), have been of interest because of their unique physical properties (*3*) and their use as cathodes in high-energy-density batteries (*4*). One unusual physical property exhibited by these materials is staging. The phenomenon of staging occurs when one layer of intercalant is inserted after every $n$th host layer to yield a stage-$n$ compound.

There are two models for staging in an intercalated host. The classical model for a stage-II material is shown in Fig. 1, where one van der Waals (vdW) gap contains the intercalated species, and the two adjacent gaps are empty. For a staging transformation to occur, it would be necessary for some of the guest species to migrate to the edge of the crystal or to penetrate through the host layer or host-layer defects to migrate to a previously unoccupied gap. In the island model of Daumas and Hérold (*5*) shown in Fig. 2, it is proposed that the

* To whom correspondence should be addressed.



0022-4596/90 $3.00

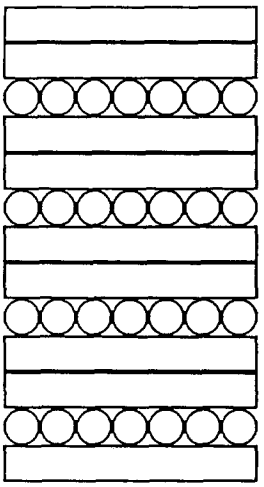

FIG. 1. Classical model for a stage-II intercalate. The blocks represent host layers and the circles depict the intercalant.

guest forms domains, or islands, within each gap of the host. For a staging transformation to occur in this model, the guest species need only migrate within the gap, and no motion perpendicular to the host layers is necessary.

Silver intercalated into titanium disulfide has received recent attention because of its two-dimensional nature, interesting staging transformations (*6, 7*), high mobility, and electron donation by silver to the conduction band of the host (*8, 9*). $Ag_xTiS_2$ intercalation compounds can be prepared electrochemically or thermally, with both preparation techniques yielding similiar single-phase regions (*8, 10, 11*) at ambient temperatures. For a mole fraction of silver ($x$) in the range of 0.15–0.25, only a stage-II compound is present, whereas for $x$ = 0.35–0.43, a stage-I compound exists. A mixed phase comprised of stage-I and stage-II compounds exists at intermediate silver concentrations. Both the stage-I and the stage-II compounds have silver located in the octahedral sites in the vdW gaps.

Silver in the $Ag_xTiS_2$ system has been demonstrated to order in an $a\sqrt{3} \times a\sqrt{3}$

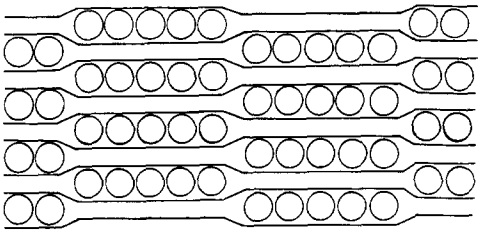

FIG. 2. Daumas–Hérold model of a stage-II intercalate. The lines represent host layers and the circles depict the intercalant.

superlattice by occupying appropriate octahedral sites in the vdW gaps at or below 300 K (*12–15*), as shown in Fig. 3. The two-dimensional, $a\sqrt{3} \times a\sqrt{3}$ superlattice for stage-II $Ag_xTiS_2$ (where $x$ is 0.16–0.18) has been observed by diffuse X-ray scattering from a single crystal (*12*) and by Raman scattering (*13*). In stage-I $Ag_{0.35}TiS_2$, the three-dimensional, $a\sqrt{3} \times a\sqrt{3} \times 2c$ superlattice has been observed by single crystal X-ray techniques (*15*).

Staging transformations can be initiated by changing the concentration of the guest species or by varying the temperature of the sample. A recent study (*6*) has been made of the phases of the $Ag_xTiS_2$ system

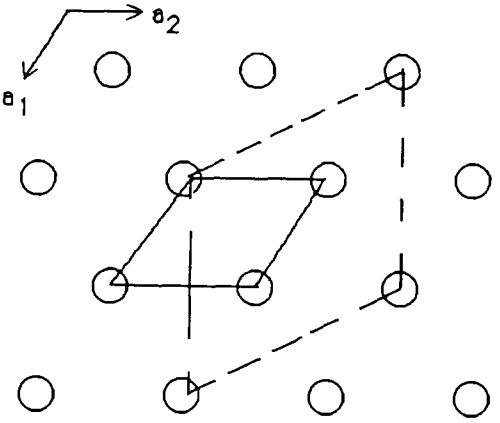


FIG. 3. Circles represent available octahedral sites for silver occupation in a partially-filled van der Waals gap. The solid line is the standard unit cell, and dotted line represents a $a\sqrt{3} \times a\sqrt{3}$ superlattice unit cell.

at elevated temperatures using X-ray powder diffraction (XPD). The phase diagram was reported for $x = 0.00–0.40$ in the temperature range 1073–1473 K. These samples were prepared by thermally intercalating an appropriate amount of silver into $TiS_2$, then annealing the compounds at the desired temperature and quenching them to ambient temperature. The XPD results for these $Ag_xTiS_2$ compounds (*6*), where $x = 0.12–0.18$, are summarized in Fig. 4. Samples quenched from temperatures up to 1173 K yielded stage-II materials. Samples which were quenched from temperatures in the range of 1223–1373 K contained a stage-disordered mixture of stage-I and stage-II phases. Samples quenched from above 1373 K were found to be entirely stage-I material.

The analysis of XPD data on quenched $Ag_xTiS_2$ samples introduces some uncertainty in the previous work (*6*). In this study, *in situ* neutron powder diffraction has been used to investigate the transition between stage-II and stage-I structures and the reversibility of this transition, which avoids the uncertainty introduced in the investigation of quenched samples.

## Experimental

Highly stoichiometric $TiS_2$ was prepared by direct reaction of the elements using 40 mg/cm$^3$ of excess sulfur at 913 K, as previously described (*16, 17*). The stoichiometry of the host prepared in this fashion is $Ti_{1.002\pm0.001}S_2$ (*17*). The silver, 99.999%, was purchased from Alfa Products. Both the host and intercalate were handled in a helium-filled Vacuum Atmospheres Model M0-40-1H dry box (<1 ppm $H_2O$ and $O_2$) and were only removed from the dry box in leak-checked, sealed containers unless otherwise noted.

Stage-II $Ag_{0.167}TiS_2$ was thermally prepared by reacting stoichiometric amounts of silver and $TiS_2$ in sealed ($<10^{-5}$ Torr) quartz ampoules at 1073 K (±1 K) for at least 100 hr. The sample was allowed to cool to ambient temperature by turning off the furnace. After cooling, no excess sulfur was found, indicating that no observable amount of titanium has cointercalated with the silver into the vdW gap.

XPD patterns were obtained on $Ag_{0.167}TiS_2$ to confirm that intercalation was complete. The patterns were collected in air using a Rigaku DMAX-IIB powder diffractometer. The intercalated sample was mounted on a quartz slide with a thin adhesive layer of petroleum jelly. The pattern was collected in a range of $2\Theta = 3–90°$ with a scan rate of 2°/min.

Time-of-flight (TOF) neutron powder diffraction data were collected on the High Intensity Powder Diffractometer (HIPD) at the Los Alamos Neutron Scattering Center at Los Alamos National Laboratory and on

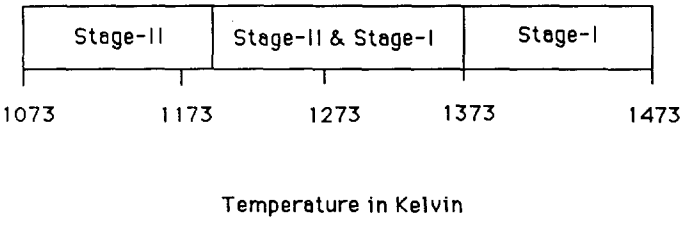


FIG. 4. Summary of staging vs temperature for $Ag_xTiS_2$, where $0.12 \leq x \leq 0.18$, reported previously (*6*) using samples quenched from the indicated temperature. Structures were determined using XPD at ambient temperature. The phase boundaries are approximate.

the General Purpose Powder Diffractometer (GPPD) at the Intense Pulsed Neutron Source at Argonne National Laboratory. Three grams of stage-II $Ag_{0.167}TiS_2$ was annealed at 1073 K for 24 hr and loaded into a vanadium sample container in a helium-filled dry box which was sealed for the HIPD study. Samples were annealed to avoid silver segregation to the edges of the crystals (*6*). The sample and the container were placed on HIPD and the sample compartment was evacuated, cooled, and maintained at 13 K during the data collection. Two more data sets were collected, first at 150 K and finally at 305 K. The sample was given several hours at each temperature to thermally equilibrate. All data sets on HIPD were collected for at least 6 hr.

A second 3-g sample of $Ag_{0.167}TiS_2$ was sealed with 50 Torr of helium in a quartz ampoule for the GPPD NPD study. This sample was annealed at 1073 K for 10 hr prior to analysis on GPPD. A small data set was collected at ambient temperature to verify the presence of pure stage-II starting material. Using the Howe furnace attachment (*18*), the temperature of the sample was raised to 1123 K and eventually to 1323 K. Again, the sample was annealed several hours at each temperature to thermally equilibrate. Data sets at 1123 and subsequently at 1323 K were collected for 20 hr each. Then the sample was allowed to cool to ambient temperature in the furnace, and a final data set was collected for 12 hr.

The NPD data were analyzed by the Rietveld method (*19*) using the Generalized Crystal Structure Analysis System (GSAS) for TOF data (*20, 21*). Initial positions for titanium, sulfur, and silver were obtained from a previous X-ray diffraction study (*8, 22*). The data from the back-scattering banks of detectors were selected for refinement. For the HIPD data, the range of 0.50–3.18 Å was used from the 153° bank. The range of data used from GPPD was 0.50–2.97 Å for the 148° bank of detectors. Atom positions, isotropic temperature factors, absorption, lattice parameters, and profile coefficients were refined for all data sets. The background for the HIPD data sets was fit with a refineable twelve-term cosine Fourier series. The background of the GPPD data sets was fitted using a radial distribution model for the peaks of quartz, as previously described (*23*).

## Results and Discussion

### *A. X-ray Characterization*

Ambient-temperature XPD patterns of stage-II $Ag_{0.167}TiS_2$ compared favorably in peak location and intensity with previous studies (*10*). In preparations where larger amounts of starting material were used, a minor phase(s) was present after the normal reaction period of 100 hr at 1073 K. The minor phase(s) was identified, by comparison of *d*-spacings, as stage-I $Ag_xTiS_2$ and/or $TiS_2$. For such samples, single-phase stage-II $Ag_{0.167}TiS_2$ was prepared by repeating the heating process for an additional 100 hr.

Samples were left for more than 2 months in sealed, evacuated quartz ampoules and showed no structural or visual signs of deintercalation. It has been previously reported that such samples partially deintercalated within 2 weeks, as observed by XPD (*6*). Although their storage procedures are not mentioned, it is now clear that such deintercalation does not occur for samples sealed under vacuum, where surface and edge oxidation/hydrolysis are minimized.

### *B. NPD Rietveld Refinement*

The TOF refinement parameters from the data collected on HIPD at 13, 150, and 305 K are given in Table I. The final difference plot for the NPD Rietveld refinement for the 150 K data is shown in Fig. 5. The atom positions and thermal factors for each refinement are given in Table II. Interatomic

TABLE I

NEUTRON TOF PARAMETERS FOR $Ag_{0.167}TiS_2$ FROM HIPD

| | 13 K | 150 K | 305 K |
|---|---|---|---|
| Space group | $P\bar{3}m1$ | $P\bar{3}m1$ | $P\bar{3}m1$ |
| Cell parameters | | | |
| $a$(Å) | 3.4057(5) | 3.4082(3) | 3.4161(4) |
| $c$(Å) | 12.033(2) | 12.056(1) | 12.100(2) |
| Detector bank (degrees) | 153 | 153 | 153 |
| Data range (msec) | | 2.515–15.989 | |
| Data range (Å) | | 0.5000–3.1787 | |
| Number of contributing reflections | 512 | 520 | 538 |
| Number of degrees of freedom | 2706 | 2690 | 2727 |
| $R_{wp}$[a] | 0.0497 | 0.0428 | 0.0552 |
| $R_p$[a] | 0.0339 | 0.0290 | 0.0374 |
| $R_e$[a] | 0.0516 | 0.0448 | 0.0575 |

[a] $R_{wp} = [\Sigma[w^*|I(\text{obsd}) - I(\text{calcd})|]^2/\Sigma[w^*I(\text{obsd})]^2]^{1/2}$. $R_p = \Sigma[|I(\text{obsd}) - I(\text{calcd})|]/\Sigma[I(\text{obsd})]$. $R_e = R_{wp}/[\chi^2]^{1/2}$, where $I$(obsd) is the observed intensity, $I$(calcd) is the calculated intensity, $w^*|I(\text{obsd}) - I(\text{calcd})|$ is the weighted difference in intensities, $\chi^2 = [\Sigma[w^*|I(\text{obsd}) - I(\text{calcd})|]^2/(N_{obs} - N_{var})]$, $N_{obs}$ is the number of profile parameters and $N_{var}$ is the number of variables. The weighting scheme is based solely on counting statistics.

TABLE II

ATOMIC POSITIONS AND THERMAL PARAMETERS FOR $Ag_{0.167}TiS_2$ AT 15, 150, AND 305 K

| $T$ (K) | Atom | $x$ | $y$ | $z$ | OCC[a] | $U_{iso}$ |
|---|---|---|---|---|---|---|
| 15 | Ag | 0 | 0 | 0 | $\frac{1}{3}$ | 0.0026(7) |
| | Ti | 0 | 0 | 0.2662(2) | 1.0 | 0.0005(5) |
| | S(1) | $\frac{1}{3}$ | $\frac{2}{3}$ | 0.1452(2) | 1.0 | 0.0019(6) |
| | S(2) | $\frac{2}{3}$ | $\frac{1}{3}$ | 0.3823(3) | 1.0 | 0.0028(5) |
| 150 | Ag | 0 | 0 | 0 | $\frac{1}{3}$ | 0.0104(9) |
| | Ti | 0 | 0 | 0.2666(3) | 1.0 | 0.0029(5) |
| | S(1) | $\frac{1}{3}$ | $\frac{2}{3}$ | 0.1449(2) | 1.0 | 0.0042(7) |
| | S(2) | $\frac{2}{3}$ | $\frac{1}{3}$ | 0.3815(3) | 1.0 | 0.0030(5) |
| 305 | Ag | 0 | 0 | 0 | $\frac{1}{3}$ | 0.024(2) |
| | Ti | 0 | 0 | 0.2677(4) | 1.0 | 0.0058(9) |
| | S(1) | $\frac{1}{3}$ | $\frac{2}{3}$ | 0.1452(4) | 1.0 | 0.006(1) |
| | S(2) | $\frac{2}{3}$ | $\frac{1}{3}$ | 0.3810(5) | 1.0 | 0.0065(8) |

[a] OCC reflects site occupancy factor.

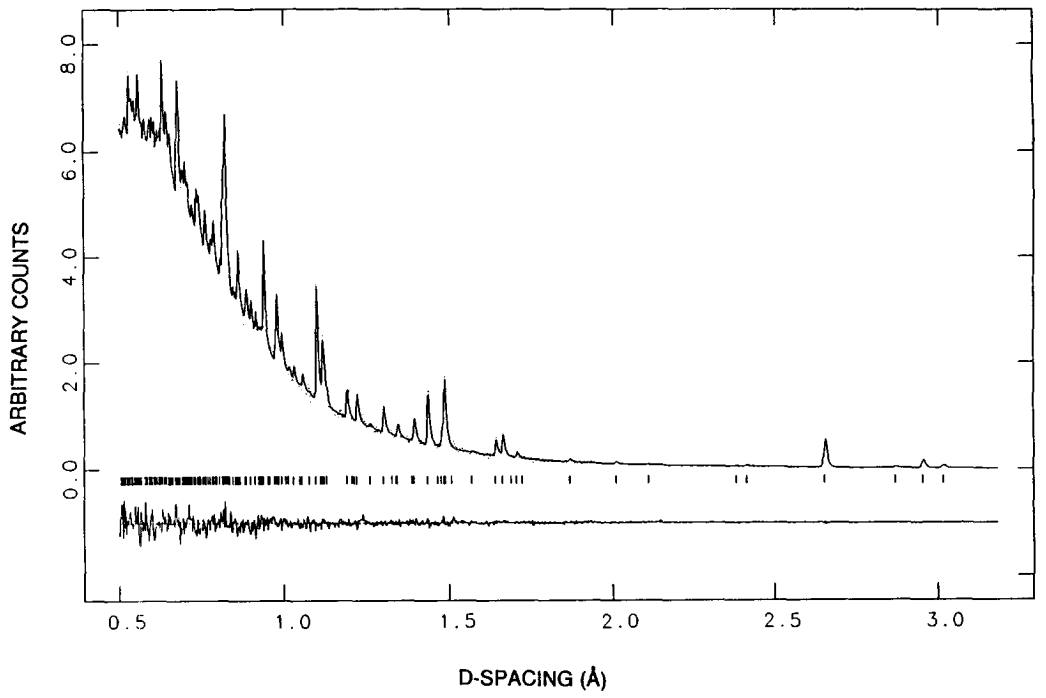


FIG. 5. Neutron counts per microsecond vs $d$-spacing of stage-II $Ag_{0.167}TiS_2$ at 150 K over the range 0.50–3.18 Å. The measured data points are denoted by dots; the Rietveld profile is the solid line fitting the observations and the difference (residual) is shown below the pattern. The tic marks represent the calculated $d$-spacings.

TABLE III

INTERATOMIC DISTANCES (Å) AND BOND ANGLES (DEG) FOR $Ag_{0.167}TiS_2$ AT 15, 150, AND 305 K

| | 13 K | 150 K | 305 K |
|---|---|---|---|
| Distance | | | |
| Ti–S(1) | 2.45(2) | 2.45(1) | 2.47(2) |
| Ti–S(2) | 2.41(2) | 2.41(1) | 2.40(2) |
| Ag . . . Ag | 3.4057(5) | 3.4082(3) | 3.4161(4) |
| Ag . . . Ti | 3.203(3) | 3.214(3) | 3.239(5) |
| Ag . . . S | 2.63(2) | 2.63(3) | 2.64(2) |
| S(1) . . . S(1) | 4.01(1) | 4.011(8) | 4.03(1) |
| S(1) . . . S(2) | 3.47(1) | 3.46(1) | 3.47(1) |
| S(2) . . . S(2) | 3.45(1) | 3.47(1) | 3.49(1) |
| Bond Angles | | | |
| S(1)–Ti–S(1) | 88.2(3) | 88.0(7) | 87.6(4) |
| S(1)–Ti–S(2) | 91.0(3) | 90.9(7) | 90.8(3) |
| S(2)–Ti–S(2) | 89.8(5) | 90.2(3) | 90.7(4) |

TABLE IV

NEUTRON TOF PARAMETERS FOR $Ag_{0.167}TiS_2$ FROM GPPD

| | 1123 K | 1323 K | 298 K |
|---|---|---|---|
| Space group | $P\bar{3}m1$ | $P\bar{3}m1$ | $P\bar{3}m1$ |
| Cell parameters | Stage-I | Stage-I | Stage-II |
| $a$(Å) | 3.4676(1) | 3.4812(2) | 3.4130(2) |
| $c$(Å) | 6.2247(4) | 6.2564(4) | 12.0924(8) |
| Detector bank (deg) | 148 | 148 | 148 |
| Data range (msec) | | 5.214–31.000 | |
| Data range (Å) | | 0.5000–2.973 | |
| Number of contributing reflections | 248 | 249 | 463 |
| Number of degrees of freedom | 1746 | 1757 | 2557 |
| $R_{wp}$[a] | 0.0250 | 0.0242 | 0.0564 |
| $R_p$[a] | 0.0170 | 0.0161 | 0.0398 |
| $R_e$[a] | 0.0159 | 0.0162 | 0.0236 |

[a] $R_{wp} = [\Sigma[w^*|I(\text{obsd}) - I(\text{calcd})|]^2/\Sigma[w^*I(\text{obsd})]^2]^{1/2}$. $R_p = \Sigma[|I(\text{obsd}) - I(\text{calcd})|]/\Sigma[I(\text{obsd})]$. $R_e = R_{wp}/[\chi^2]^{1/2}$, where $I$(obsd) is the observed intensity, $I$(calcd) is the calculated intensity, $w^*|I(\text{obsd}) - I(\text{calcd})|$ is the weighted difference in intensities, $\chi^2 = [\Sigma[w^*|I(\text{obsd}) - I(\text{calcd})|]^2/(N_{obs} - N_{var})]$, $N_{obs}$ is the number of profile parameters and $N_{var}$ is the number of variables. The weighting scheme is based solely on counting statistics.

distances and bond angles are reported in Table III. All peaks in each data set are indexed to stage-II $Ag_{0.167}TiS_2$, with the silver atoms being located in the octahedral sites in the vdW gaps. The silve mole fraction was determined from the initial stoichiometric concentration and was not refined.

The TOF refinement parameters from the data collected on GPPD progressively at 1123, 1323, and 298 K are given in Table IV. All peaks in the 298 K data set are indexed to a stage-II material, with the silver atoms located in the octahedral sites in the vdW gaps. In the two higher-temperature data sets, all peaks are indexed to a stage-I material, with silver located in the octahedral sites. The final difference plot for the Rietveld refinements for the data set at 1323 K is shown in Fig. 6. The atom positions and thermal factors for each data set are reported in Table V, with the interatomic distances and bond angles summarized in Table VI.

Titanium disulfide consists of a hexagonal arrangement of metal atoms sandwiched between two hexagonally closest-packed sulfur layers, with the titanium located in octahedral sites. The $TiS_2$ layer is believed to remain essentially unchanged during intercalation. In stage-II $Ag_{0.167}TiS_2$ the distance spanned by the host sulfur lay-

TABLE V

ATOMIC POSITIONS AND THERMAL PARAMETERS FOR $Ag_{0.167}TiS_2$ AT 1123, 1323, AND 298 K

| $T$ (K) | Atom | $x$ | $y$ | $z$ | OCC[a] | $U_{iso}$ |
|---|---|---|---|---|---|---|
| 1123 | Ag | 0 | 0 | 0 | $\frac{1}{6}$ | 0.170(9) |
| | Ti | 0 | 0 | 0.5 | 1.0 | 0.060(2) |
| | S | $\frac{1}{3}$ | $\frac{2}{3}$ | 0.2738(6) | 1.0 | 0.054(2) |
| 1323 | Ag | 0 | 0 | 0 | $\frac{1}{6}$ | 0.20(1) |
| | Ti | 0 | 0 | 0.5 | 1.0 | 0.065(3) |
| | S | $\frac{1}{3}$ | $\frac{2}{3}$ | 0.2766(6) | 2.0 | 0.057(3) |
| 298 | Ag | 0 | 0 | 0 | $\frac{1}{3}$ | 0.022(2) |
| | Ti | 0 | 0 | 0.2661(6) | 1.0 | 0.0010(9) |
| | S(1) | $\frac{1}{3}$ | $\frac{2}{3}$ | 0.1452(5) | 1.0 | 0.0020(7) |
| | S(2) | $\frac{2}{3}$ | $\frac{1}{3}$ | 0.3807(7) | 1.0 | 0.0020(7) |

[a] OCC reflects site occupancy factor.

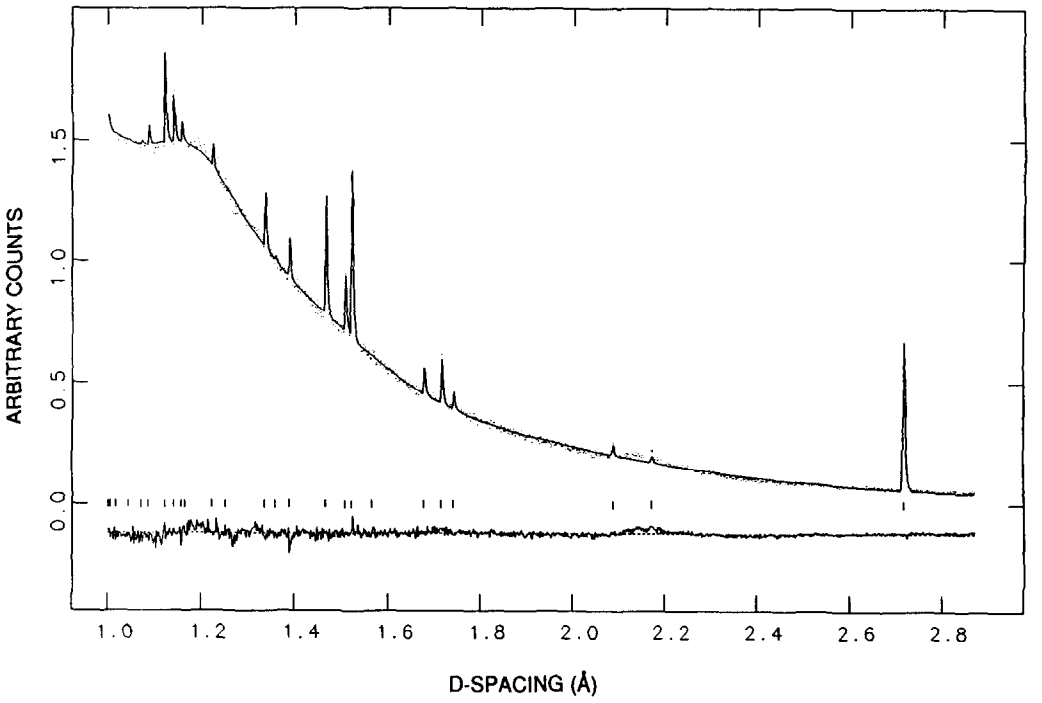


FIG. 6. Neutron counts per microsecond vs $d$-spacing of stage-I $Ag_{0.167}TiS_2$ at 1323 K over the range 1.00–2.87 Å. The measured data points are denoted by dots; the Rietveld profile is the solid line fitting the observations and the difference (residual) is shown below the pattern. The tic marks represent the calculated $d$-spacings.

ers (2.85 ± 0.01 Å) about the titanium layer is indeed quite similiar to the value of 2.84 Å observed for $TiS_2$ at ambient temperature (*24*), as shown in Fig. 7, yet the distances between the titanium layer and the two adjoining sulfur layers are no longer equal. The distance between the Ti and S(1) layers, where S(1) is the layer that is closest to the vdW gap which contains the silver, is larger than the distance between the Ti and S(2) layers, as illustrated in Fig. 7. Therefore, although the sulfur positions surrounding the titanium do not change significantly from their closest-packed arrangement in $TiS_2$, the titanium position does. Here, Ti has the same $x$ and $y$ coordinates as Ag and has moved away from the center of the host-sulfur trigonal antiprism along ⟨001⟩ due to the Coulombic repulsion between titanium and silver. In contrast, stage-I $Ag_{0.167}TiS_2$ does not exhibit any Ti displacement from the host-layer midplane because the Coulombic interactions between titanium and silver are symmetrical. Moreover, for stage-II $Ag_{0.167}TiS_2$, the unoccupied vdW gap expands with increasing temperature, which is probably associated with increased thermal motion. The distance between the Ti and S(1) layers increases slightly with temperature and the distance between the Ti and S(2) layers decreases such that the total distance spanned by the host sulfur layers remains nearly constant. This behavior occurs because the sulfur atoms in the $a_1$–$a_2$ plane move further apart as the temperature is increased (as shown by the increased $a$ lattice parameter) which allows the titanium to move further from the silver (see Table III). The host-layer bond angles for both stage-I and

TABLE VI

INTERATOMIC DISTANCES (Å) AND BOND ANGLES (DEG) FOR $Ag_{0.167}TiS_2$ AT 1123, 1323, AND 298 K

| | 1123 K | 1323 K | 298 K |
|---|---|---|---|
| Distance | | | |
| Ti–S | 2.448(2) | 2.448(7) | 2.453(7) |
| | [e] | [e] | 2.409(8) |
| Ag . . . Ag | 3.4676(2) | 3.4812(2) | 3.4130(2) |
| Ag . . . Ti | 3.1124(2) | 3.1282(2) | 3.218(7) |
| Ag . . . S | 2.629(3) | 2.652(3) | 2.639(4) |
| S(1) . . . S(1)[a] | 3.953(7) | 4.002(8) | 4.03(1) |
| S(1) . . . S(1)[b] | 3.455(6) | 3.443(7) | — |
| S(1) . . . S(2) | [e] | [e] | 3.463(7) |
| S(2) . . . S(2) | [e] | [e] | 3.49(1) |
| Bond Angles | | | |
| S(1)–Ti–S(1)[c] | 90.0(1) | 90.6(1) | 88.1(3) |
| S(1)–Ti–S(1)[d] | 90.0(1) | 89.4(2) | |
| S(1)–Ti–S(2) | [e] | [e] | 90.8(3) |
| S(2)–Ti–S(2) | [e] | [e] | 90.2(4) |

[a] Spans $TiS_6$ octahedra for stage-I structure.

[b] Spans $AgS_6$ octahedra for stage-I structure.

[c] Sulfur atoms in same sulfur plane for stage-I structure.

[d] Sulfur atoms in sulfur planes adjacent to the titanium plane for stage-I structure.

[e] Stage-I intercalate has only one type of sulfur.

stage-II $Ag_{0.167}TiS_2$ are similar to the $TiS_2$ values which have been discussed in earlier work (*24*).

### C. *Phase Analysis*

Superstructure formation in stage-II $Ag_{0.167}TiS_2$ was not observed by NPD upon cooling to 13 K. However, an $a\sqrt{3} \times a\sqrt{3}$ superstructure has been observed previously near 300 K or below by diffuse X-ray single crystal diffraction (*12*) and by Raman scattering (*13*). This two-dimensional $a\sqrt{3} \times a\sqrt{3}$ superstructure would appear as columns in the $c^*$ direction in reciprocal space, and these columns would have little intensity observable to NPD. Hence, the absence of superstructure in the NPD data is consistent with two-dimensional $a\sqrt{3} \times a\sqrt{3}$ ordering.

The high-temperature structural study of $Ag_{0.167}TiS_2$ has shown that the transition from a stage-II to a stage-I structure occurs at a temperature below the temperature range of 1200–1373 K reported previously (*6*). The transition to a stage-I material upon heating, which has been reported to be irreversible (*6*), was shown by NPD to be reversible upon slow cooling yielding the original stage-II compound. This high-temperature NPD study demonstrates that quenching a sample from a high temperature does not necessarily "lock in" the higher-temperature phase, as previously assumed (*6*).

When samples of stage-I $Ag_{0.167}TiS_2$ were quenched to ambient temperatures from 1300 K sulfur was observed to have separated from the intercalate. This behavior is enhanced by the higher temperature of the intercalate relative to the ampoule wall during quenching. This sulfur loss is probably accompanied by the migration of titanium ($Ti^{4+}$) from the host lattice into the vdW gap. A second sample of $Ag_{0.167}TiS_2$ was allowed to slowly cool from this high temperature and all the sulfur recombined with the lattice. XPD patterns were collected from both samples in the manner described previously. The slowly cooled sample was identified as stage-II $Ag_{0.167}TiS_2$, whereas the quenched material yielded a stage-disordered mixture of stage-I and stage-II $Ag_{0.167}TiS_2$, as observed in previous work (*6*). A possible explanation for the presence of the two stages is incomplete quenching, with the material nearest the surface cooling rapidly and probably "locking" in a stage-I structure, whereas material in the interior of the ampoule cools more slowly and converts to the stage-II structure.

The isotropic thermal parameters for all temperatures observed above 15 K indicate that titianium and sulfur exhibit relatively little thermal motion compared to Ag (see

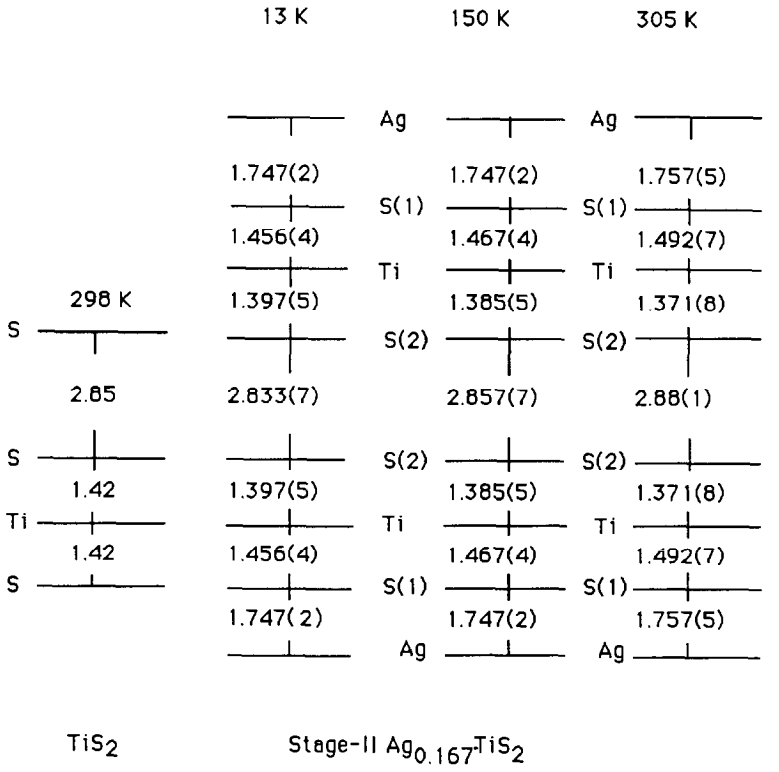


FIG. 7. Comparison of layer separations for stage-II $Ag_{0.167}TiS_2$ and $TiS_2$ (*24*).

Tables II and V). This follows from the relatively strong Ti–S bonding within a host layer compared to weaker Ag guest-host bonding, plus the motion of silver over several octahedral sites. This data did not support the refinement of anisotropic thermal parameters, but $U_{11}$ would be expected to be larger than $U_{33}$, similar to Ag in other layered compounds (*25*).

## Conclusions

Superstructure formation was not observed for stage-II $Ag_{0.167}TiS_2$ upon cooling to 13 K, consistent with previous observations of a $a\sqrt{3} \times a\sqrt{3}$ two-dimensional superstructure (*12* and *13*). However, structural evidence has been obtained for significant Coulombic repulsive interactions between titanium and silver in this compound.

The high-temperature structural study of $Ag_{0.167}TiS_2$ has demonstrated that the transition from a stage-II compound to a stage-I material is reversible and occurs at a lower temperature than reported previously (*6*). This investigation shows that a sample quenched from high temperatures does not necessarily "lock in" the high-temperature structure, as previously assumed (*6*). Therefore, the stage-I/stage-II two-phase region of the high-temperature phase diagram reported in the literature (*6*) can be attributed to incomplete quenching. Furthermore, quenching of these intercalates from high temperatures may enhance the loss of host-layer sulfur and concomitant intercalation of $Ti^{4+}$ into the vdW gap (*26*).

## Acknowledgments

This study has benefited from the use of LANSCE at Los Alamos National Laboratory and IPNS at Argonne National Laboratory. IPNS is funded by the Department of Energy, BES-Materials Science, under Contract W-31-109-Eng-38. We thank R. L. Hitterman at IPNS and A. Williams and A. C. Lawson at LANSCE for assistance in data collection and G. A. Wiegers for helpful conversations. We are grateful to the National Science Foundation for support through Grant DMR-8605937, Arizona State University for the necessary computer time and the use of the X-ray facilities, the Center for Solid State Science at Arizona State University for the use of its Materials Preparation Facility, and M. Wheeler and W. O'Neill for expert assistance in glassblowing.

## References

1. M. S. WHITTINGHAM, *Prog. Solid State Chem.* **12,** 41 (1978).
2. R. H. FRIEND AND A. D. YOFFE, *Adv. Phys.* **36,** 1 (1987).
3. A. D. YOFFE, *Solid State Ionics* **9/10,** 59 (1983).
4. M. S. WHITTINGHAM, *J. Solid State Chem.* **29,** 303 (1979).
5. N. DAUMAS AND A. HÉROLD, *C.R. Acad. Sci. Ser. C* **268,** 373 (1969).
6. K. K. BARDHAN, G. KIRCZENOW, G. JACKLE, AND J. C. IRWIN, *Phys. Rev. B* **33,** 4149 (1985).
7. G. A. WIEGERS, H. J. M. BOUWMEESTER, AND A. G. GERARDS, *Solid State Ionics* **16,** 155 (1985).
8. A. G. GERARDS, H. ROEDE, R. J. HAANGE, B. A. BOUKAMP, AND G. A. WIEGERS, *Synth. Met.* **10,** 51 (1984/85).
9. D. KALUARACHCHI AND R. F. FRINDT, *Phys. Rev. B* **31,** 3648 (1985).
10. G. A. SCHOLZ AND R. F. FRINDT, *Mater. Res. Bull.* **15,** 1703 (1980).
11. J. SCHRAMKE AND R. SCHÖLLHORN, *Solid State Ionics* **23,** 197 (1987).
12. K. OHSHIMA AND S. C. MOSS, *Acta Crystallogr. Sect A* **39,** 298 (1983).
13. W. K. UNGER, J. M. REYES, O. SINGH, A. E. KURZON, J. C. IRWIN, AND R. F. FRINDT, *Solid State Commun.* **28,** 109 (1978).
14. R. LEONELLI, M. PLISCHKE, AND J. C. IRWIN, *Phys. Rev. Lett.* **45,** 1291 (1980).
15. G. A. WIEGERS, K. D. BRONSEMA, S. VAN SMAALEN, R. J. HAANGE, J. E. ZONDAG, AND J. L. DE BOER, *J. Solid State Chem.* **67,** 9 (1987).
16. L. BERNARD, M. MCKELVY, W. GLAUNSINGER, AND P. COLOMBET, *Solid State Ionics* **15,** 301 (1985).
17. M. J. MCKELVY AND W. S. GLAUNSINGER, *J. Solid State Chem.* **66,** 181 (1987).
18. "IPNS Progress Report 1986–1988" (F. J. Rotella, Ed.), Vol. 20, Argonne National Laboratory.
19. H. M. RIETVELD, *J. Appl. Crystallogr.* **2,** 65 (1965).
20. A. C. LARSON AND R. B. VON DREELE, "Generalized Crystal Structure Analysis System," Los Alamos National Laboratory, LAUR 86-748 (1986).
21. R. B. VON DREELE, J. D. JORGENSEN, AND C. B. WINDSOR, *J. Appl. Crystallogr.* **15,** 581 (1982).
22. M. MORI, K. OHSHIMA, S. C. MOSS, R. F. FRINDT, M. PLISCHKE, AND J. C. IRWIN, *Solid State Commun.* **43,** 781 (1982).
23. A. C. LAWSON, B. CORT, C. E. OLSEN, J. W. RICHARDSON, M. H. MUELLER, G. H. LANDER, J. A. GOLDSTONE, A. WILLIAMS, G. H. KWEI, R. B. VON DREELE, J. FABER, JR., AND R. L. HITTERMAN, "Advances in X-ray Analysis" (C. S. Barrett *et al.*, Eds.), Vol. 31, p. 385, Plenum, New York (1988).
24. R. R. CHIANELLI, J. C. SCANLON, AND A. H. THOMPSON, *Mater. Res. Bull.* **10,** 1379 (1975).
25. F. M. R. ENGELSMAN, G. A. WIEGERS, F. JELLINEK, AND B. VAN LAAR, *J. Solid State Chem.* **6,** 574 (1973).
26. A. H. THOMPSON, F. R. GAMBLE, AND C. R. SYMON, *Mater. Res. Bull.* **10,** 915 (1975).